Comparison of MPR-based flooding methods in different environments

JAN NILSSON OCH ULF STERNER

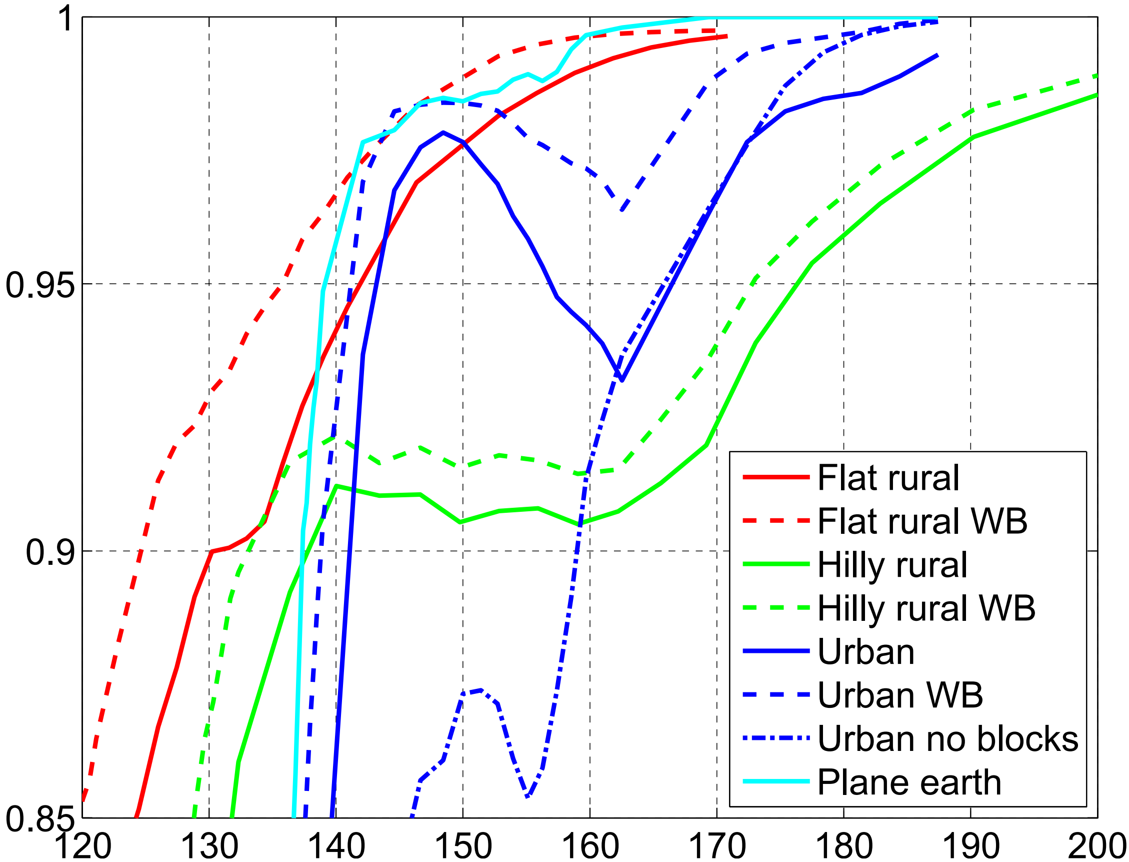

FOI-R--3701--SE
ISSN 1650-1942 June 2013

Jan Nilsson och Ulf Sterner

Comparison of MPR-based flooding methods in different environments

Titel	Jämförelse av MPR-baserade flödningsmetoder i olika miljöer
Title	Comparison of MPR-based flooding methods in different environments
Rapportnr / Report No.	FOI-R--3701--SE
Månad / Month	Juni / June
Utgivningsår / Year	2013
Antal sidor / Pages	48
ISSN	1650-1942
Kund / Customer	FMV
Forskningsområde	4. Informationssäkerhet och kommunikation
FoT område	Ledning och MSI
Projektnr / Project No.	E323431
Godkänd av / Approved by	Christian Jönsson
Ansvarig avdelning	Informations- och aerosystem

Abstract

The aim is to achieve robust broadcasting and the paper explores how the propagation environment affects different MPR-based broadcast methods. There are several methods, or combinations of methods, that can be used to increase the robustness of MPR-based flooding. As a reference we consider the basic MPR selection method in OLSR, called MPR-default, and investigate the use of physical layer information and additional MPRs. It is also important to consider the cost of implementing these methods. To investigate which method to choose, a channel model that mimics real radio transmissions is employed. We consider an urban, a flat plain and a hilly forest environment. The results show, among other things, that the choice of method depends on the dynamics of the channel and the network connectivity. The MPR-default method does not give enough robustness, except when the mobility is low and the environment is flat, so other methods are required. For sparse networks, using additional MPRs is a good choice, but for dense networks, using physical layer information and a fading margin is more efficient.

Keywords: MPR-based flooding, channel model, different environments, ad hoc networks

Sammanfattning

I rapporten undersöker vi metoder för hur man effektivt kan åstadkomma robust MPR-baserad broadcast i mobila taktiska ad hoc-nät. Speciellt utforskar vi hur olika utbredningsmiljöer påverkar olika MPR-baserade metoders prestanda. Det finns flera olika metoder, eller kombinationer av metoder som kan avvändas för att öka robustheten hos MPR-baserad broadcast. Vi studerar standardmetoden i OLSR för att välja MPR-noder, MPR-default, som en referens och undersöker användande av fysik lager information och att lägga till ytterligare MPR noder. Viktigt är också att beakta komplexiteten för att implementera metoderna. För att undersöka vilken metod som bör väljas används en kanalmodell med vars hjälp olika utbredningsmiljöer kan efterliknas. Vi analyserar prestanda för stadsmiljö och några olika landsbyggdmiljöer såsom slättmark och skogsterräng. Resultaten visar på att hur bra en metod fungerar beror av topologin och framförallt dynamiken i nätet, d v s hur snabbt länkarna mellan noderna ändras. MPR-default är inte tillräckligt robust, utom möjligen i en platt miljö, så andra metoder krävs. För glesa nät är metoden att lägga till ytterligare MPR noder ett bra alternativ, men för väl förbundna nät är det mera effektivt att använda fysisk lager information.

Nyckelord: MPR-baserad flödning, kanalmodell, olika miljöer, ad hoc-nät

Contents

1 Introduction

Much of the traffic in tactical ad-hoc networks is of broadcast (or multicast) nature. Examples of broadcast applications are position and information sharing situational awareness (SA) data, orders and Push-To-Talk (PTT) voice communications. Mobility means that rapid topology changes may occur in tactical ad hoc networks, i.e., links frequently go up and down and connectivity may suddenly rely on a few long and weak links. In such situations, achieving reliable broadcasting at low cost, i.e., low overhead, is a challenge.

The simplest and most robust way to broadcast is by flooding. Then all nodes relay every packet but flooding suffers from high overhead. In many cases, however, reliable broadcasting can be achieved by selecting only a subset of the nodes as relays. The issue is which nodes to select. One of the most popular ways of selecting the relays is to use the multi-point-relay MPR method according to the Simplified Multicast Forwarding (SMF) framework [1], and the MPR selection mechanisms in OLSR [2].

Many papers have investigated and proposed improvements to the MPR selection mechanism in OLSR, e.g.,[3],[4]. However, the cost of introducing these improvements is not as well researched. Mobility as a challenge to OLSR is addressed in [5, 6]. In [7] two MPR selection alternatives are investigated for PTT and SA data. To assist in the MPR selection process, one method using lower-layer physical information in terms of the Bit Error Rates (BER) on the links, is investigated in [8]. There is a discrepancy between the results of MPR-based flooding obtained by simulations and in practical trails. A main reason is that the channel/link models used in most of the simulations are too simplistic and do not model the dynamics of the channel well enough [9, 10]. According to [10], it is now commonly accepted that better channel models, than the so-called unit disk graph model, are needed in the simulations to obtain results that reflect real radio transmission. In [10] they use the "lognormal shadowing channel model" and investigate some different MPR selection strategies. One of their findings is that the unit disk graph channel model can produce misleading results compared with using a more realistic channel model. However, node mobility is not included in the investigation.

The main contribution of this report is to investigate the performance of different broadcast alternatives using MPR-based relay sets in different environments. The channel models used have the capability to mimic real radio transmissions between nodes on the move. In particular, the channel characteristic is correlated for packets sent between two nodes as long as the positions of the nodes have not changed too much. The gains that can be obtained by using lower physical layer information for the MPR selections are also of interest. Again, it is important that the channel is modeled accurately to be able to assess the obtainable gains by using physical layer information. In [11] we examined the performance of MPR selection methods based on an urban environment. In this report we extend the results from [11] to include more types of environments.

The report is organized as follows: In Chapter 2 the principles and methods for

This work was supported by the FMV research project "Robust Multicast for tactical mobile networks", which is funded by the R&D programme of the Swedish Armed Forces.

broadcasting are described. Chapter 3 describes the propagation/channel model. In Chapter 4 statistical channel parameters for the environments used in the evaluation are presented. Chapter 5 describes the system, scenario and simulation setup. How individual propagation parameters affect the performance of MPR-based flooding is researched in Chapter 6. In Chapter 7 the main results are presented. That is, the comparison of different MPR-based methods in different environments. These results is further discussed in Chapter 8. Finally, the conclusions are presented in Chapter 9.

2 MPR Selection Methods

Optimized Link State Routing (OLSR) is a proactive ad-hoc routing protocol that has reached the status of RFC and is extensively reported in the literature. For broadcasting it is the multipoint Relay (MPR) mechanism of OLSR, originally designed for spreading topology control (TC) messages, that is of interest.

The basic idea is that each node chooses a subset of its one-hop neighbors as multipoint relays (MPR) which are the only nodes that will retransmit a message. The MPRs are chosen so that all two-hop neighbors of a node will be reached if all its MPRs retransmit a message. To select the MPRs a node requires updated information about its two-hop neighborhood. To keep track of the local neighborhood of the node HELLO messages are used. A HELLO message is transmitted to the one-hop neighbors of a node and includes a list of the node's neighbors. In this way, all nodes will be given information about the neighbors of its neighbors, that is, its two-hop neighborhood.

The MPR selection algorithm described in the OLSR RFC 3626 [2] includes many parameters and options that can be used to adjust the robustness of the algorithm. We choose to focus on three basic principles: sending more HELLO messages; demanding that the links used are reliable; and electing additional redundant MPR nodes. Furthermore, we also investigate one non-standard modification of the OLSR algorithm, called relay assistance, where nodes are allowed to elect themselves as MPR nodes if the topology information is considered unreliable. Before describing the principles studied in greater depth, we first present the default MPR algorithm which we use as the basis for all the MPR algorithms studied.

As a starting point for our modifications we use the algorithm described in the OLSR RFC 3626 [2]. As only broadcasting is treated no TC messages are considered, i.e., TC messages are not needed for broadcasting. Besides this modification the MPR-default algorithm uses OLSR RFC 3626 with default values on all parameters and no options enabled. The default setup used for the MPR-algorithm, denoted by *MPR-default*, and all the settings that are evaluated are summarized in Table 2.1.

One technique for improving MPR-default in dynamic scenarios is to send HELLO messages more frequently. Besides the default value of 2.0 seconds we have investigated the effect of using a HELLO message emission intervals of 4.0, 1.0, 0.5, and 0.25 seconds in [11]. The conclusion was that a short HELLO emission interval is not sufficient in order to obtain robust broadcasting. In this paper we only consider the

	MPR-default	Evaluated settings
OLSR link hysteresis	none	none, basic, SNR$\{\gamma_m\}$
fading margin, γ_m	–	1, 2, 4
MPR coverage	1	1, 2, 4, 8
MPR relay assistance	off	on, off

Table 2.1: Default setting and evaluated setting for the MPR algorithm.

default value of 2.0 seconds.

Note that in the extreme, when all nodes are selected as MPRs, full flooding is preferable. Full flooding needs little (if any) other type of overhead traffic than the retransmissions while MPR-based flooding also has to send the HELLO messages.

2.1 Fading/SNR Margin

To increase the robustness of MPR-based flooding the OLSR RFC used includes an optional link hysteresis framework, which lets the MPR selection algorithm consider the reliability of the links when selecting the MPR nodes. This means that only the *reliable* links are considered in the the MPR selection process.

The OLSR RFC used also includes a basic model that based solely on the HELLO messages tries to estimate the reliability of a link. If the default parameters are used for the algorithm, it will consider a new link as reliable if three consecutive HELLO messages are received. However, if one packet is lost on a reliable link the link will be considered unreliable.

The link hysteresis framework used in the OLSR RFC is open to other models for estimating the reliability of a link. Besides the basic model we will here also consider a model based on Signal-to-Noise Ratio (SNR) estimates from the lower/physical layer. We assume here that a packet can be received by the physical layer if SNR $> \gamma_0$. However to consider a link as reliable we demand that SNR $> \gamma_0\gamma_m$, where γ_m is a fading margin we use to increase the reliability of the links. We choose to base our estimates of link reliability on all packets that are detected on a link, i.e. if SNR $<$ $\gamma_0\gamma_m$ for packet on a link the link will be considered unreliable.

In the evaluation we denote this estimating method with SNR$\{\gamma_m\}$, where γ_m is the fading margin used. In our simulations we will study γ_m set to 1, 2, and 4. The case of $\gamma_m = 1$ means that we do not require any extra link reliability to start using a link. However the information from the lower/physical layer will be used to immediately remove the link when it is considered as unreliable due to low SNR. More precisely, when an anticipated packet cannot be received correctly. To obtain this information is here simplified due to a TDMA structure (see Section 5)

2.2 Additional MPRs

The basic MPR selection mechanism of the OLSR algorithm tries to minimize the MPR set in order to reduce the protocol overhead. However, by introducing redundancy in the MPR set the robustness of the algorithm can be increased at the cost of higher protocol overhead. The RFC studied allows the redundancy degree to be controlled by the MPR coverage parameter. The parameter specifies how many MPRs a 2-hop neighbor should, if possible, be reached by. In our simulations we study MPR coverage parameters set to 1, 2, 4, and 8.

2.3 Relay Assistance

An alternative approach to increasing the robustness of MPR-based flooding is to allow a node to elect itself as an extra temporary MPR if it is not already selected and the information in the topology database can be considered as unreliable for the moment. We choose here to consider the information in the topology database of a node, n_A, unreliable if the node n_A receives a packet from another node n_B and n_B has not yet announced node n_A in its HELLO messages as a symmetric neighbor.

The rule used is rather conservative and can lead to that the topology being considered incorrect in situations where the current MPR set is functioning satisfactorily. However, if robustness is the overall aim, it might be a reasonable choice. Furthermore, we choose to apply this rule on a packet-per-packet basis, i.e. the node decides whether it should select itself as an MPR for each packet it receives based on the rule above.

3 Urban Channel Model

To model the behavior of the radio channel in an urban environment we use a reduced version of the channel model in [12]. The reduced model includes different channel parameters as the variance of the the large-scale fading, the Ricean K-factor for the small-scale fading process and the coherence bandwidth of the channel. It also incorporates parameters for spatial correlation of the channel. This means that the channel characteristic is correlated for two packets sent over the same link between two nodes as long as the positions of the two nodes have not changed to much, see [12]. Including such correlations in the model is very important for the model to mimic a reality-like channel behavior.

In the original model the coherence bandwidth W_{cho} and Rician K-factor is modeled as a stochastic process. However, in the reduced model both parameters are modeled as constants. Thus, the parameter set for the model is also reduced. The structure of the reduced model is presented in this chapter. The model consists of three parts, a distance dependent part, a model of the large-scale fading process and a model of the small scale fading process.

3.1 Distance-Dependent Path Gain

The distance-dependent path-gain $G_d(d)$ is modeled to be a function of the distance d between the transmitter and receiver as

$$G_{\mathrm{d}}(d) = G_0 - 10\,n\log_{10}\left(\frac{d}{d_{\mathrm{ref}}}\right) \quad [\mathrm{dB}] \tag{3.1}$$

where G_0 is the path gain at reference distance d_{ref} and n is the path-gain exponent.

3.2 Large-Scale Fading

The large-scale fading process $G_{\mathrm{LS}}(\mathbf{r}_{\mathrm{Tx},p}, \mathbf{r}_{\mathrm{Rx},p})$, where $\mathbf{r}_{\mathrm{Tx},p}$ is the pth position for the transmitter, and $\mathbf{r}_{\mathrm{Rx},p}$ is the pth position for the reviver, is defined as

$$G_{\mathrm{LS}} = \overline{G}_{\mathrm{LS}} + \widetilde{G}_{\mathrm{LS}} \;\; [\mathrm{dB}]. \tag{3.2}$$

The first term, $\overline{G}_{\mathrm{LS}}$, is a process that varies at a quite large spatial scale, typically it can be considered as constant over one block in an urban scenario. It is only used in urban environments. The second term, $\widetilde{G}_{\mathrm{LS}}$, is a process that depends mainly on the local environment in vicinity of the radio nodes. Thus, its spatial scale is considerably smaller. However, this term is included for all environments, besides when the plane earth model is used.

The terms in equation (3.2) are only dependent of the relative movement of the transmitter and the receiver. As a measure of the relative movement of the transmitter and the receiver between the ith position and the jth position we define $\Delta_{i,j}$ as

$$\Delta_{i,j} = |\mathbf{r}_{\mathrm{Tx},i} - \mathbf{r}_{\mathrm{Tx},j}| + |\mathbf{r}_{\mathrm{Rx},i} - \mathbf{r}_{\mathrm{Rx},j}|. \tag{3.3}$$

A sequence of realizations of the large-scale fading process $\overline{G}_{\mathrm{LS}}(\mathbf{r}_{\mathrm{Tx},p}, \mathbf{r}_{\mathrm{Rx},p})$, further denoted with $\overline{G}_{\mathrm{LS}}(\cdot_p), p = 1, 2, ..., P$, is generated as

$$\overline{G}_{\mathrm{LS}}(\cdot_p) = \begin{cases} \overline{G}_{\mathrm{LS}}(\cdot_{p-1}) & \text{if } p \geq 2 \text{ and } \Delta_{k,p} < (\Delta d)_{\overline{G}_{\mathrm{LS}}} \\ \overline{\Omega}_p & \text{if } p \geq 2 \text{ and } \Delta_{k,p} \geq (\Delta d)_{\overline{G}_{\mathrm{LS}}} \\ \overline{\Omega}_p & \text{if } p = 1 \end{cases}$$

where k is the last index for which a new random variable $\overline{\Omega}_p$ was generated, $(\Delta d)_{\overline{G}_{\mathrm{LS}}}$ is the large scale correlation distance, and $\overline{\Omega}_p$ is a normal distributed variable with zero mean and variance $\sigma^2_{\overline{G}_{LS}}$.

The process $\widetilde{G}_{\mathrm{LS}}$ is also modeled as a normal distributed process. We assume that the autocorrelation function for the process can be modeled by an exponential function. Hence, a sequence of spatially correlated realizations of the large-scale fading, $\widetilde{G}_{\mathrm{LS}}(\mathbf{r}_{\mathrm{Tx},p}, \mathbf{r}_{\mathrm{Rx},p})$, further denoted with $\widetilde{G}_{\mathrm{LS}}(\cdot_p), p = 1, 2, ..., P$, is generated as

$$\widetilde{G}_{\mathrm{LS}}(\cdot_p) = \begin{cases} \alpha_p \widetilde{G}_{\mathrm{LS}}(\cdot_{p-1}) + \sqrt{1-\alpha_p^2}\,\widetilde{\Omega}_p & \text{if } p \geq 2, \\ \widetilde{\Omega}_p & \text{if } p = 1, \end{cases}$$

where $\widetilde{\Omega}_p$ is a Gaussian distributed variable with zero mean and variance $\sigma^2_{\widetilde{G}_{\mathrm{LS}}}$, and α_p a coefficient that determines the statistical dependency between $\widetilde{G}_{\mathrm{LS}}(\cdot_p)$ and $\widetilde{G}_{\mathrm{LS}}(\cdot_{p-1})$. Based on our exponential autocorrelation assumption, we model the coefficient α_p as a function

$$\alpha_p = \rho(\Delta_{p,p-1}) = \left(\frac{1}{c}\right)^{-\frac{\Delta_{p,p-1}}{(\Delta d)_{\widetilde{G}_{\mathrm{LS}}}}} \tag{3.4}$$

where $(\Delta d)_{\widetilde{G}_{\mathrm{LS}}}$ is the correlation distance at correlation level c for the large scale fading.

3.3 Small-Scale Fading

Modern radio system can usually take advantage of multipath propagation and obtain diversity gains on frequency selective channels. Therefore, the performance of modern wideband radio systems depends mainly on the instantaneous signal-to-noise ratio (SNR), averaged over the system bandwidth. The small-scale fading process is modeled as m independently fading sub-channels, where m is the diversity order of the system. We assume here that m that can be extracted by an idealized receiver can be approximated as

$$m = W_{\mathrm{s}}/W_{\mathrm{coh}}, \tag{3.5}$$

where W_{s} is the system bandwidth and W_{coh} the coherence bandwidth of the channel.

We model each of the sub-channels as a Rician distributed process, $Y\left(\mathbf{r}_{\mathrm{Tx},p}, \mathbf{r}_{\mathrm{Rx},p}\right)$, further denoted with $Y\left(\cdot_p\right)$. Furthermore we assume that the autocorrelation function can be modeled as an exponential function. Hence, a sequence of spatially correlated realizations of the Rician process, $Y\left(\cdot_p\right)$, $p = 1, 2, ..., P$, is generated as

$$Y(\cdot_p) = \begin{cases} \beta_p Y(\cdot_{p-1}) + \sqrt{1-\beta_p^2}\,\Psi_p & \text{if } p \geq 2, \\ \Psi_p & \text{if } p = 1, \end{cases} \tag{3.6}$$

where Ψ_p is Rician stochastic variable generated according to

$$\Psi_p = \sqrt{\frac{K}{K+1}} + \sqrt{\frac{1}{K+1}} X_p$$

where X_p is a complex Gaussian stochastic variable with zero means and unit variance. The parameter K (Riciean K-factor) takes values between zero and infinity and determines the fraction of energy in the direct path. It is zero when no direct path exists, and large when the direct path contains most of the energy. Furthermore, we model the coefficient β_p in the same way as α_p in equation (3.4) but with large-scale correlation distance, $(\Delta d)_{\widetilde{G}_{\mathrm{LS}}}$, replaced with the small-scale correlation distance, denoted with $(\Delta d)_{\mathrm{SS}}$.

The instantaneous SNR is then obtained from the wide band path-gain $G_{\mathrm{wb}}(\mathbf{r}_{\mathrm{Tx}}, \mathbf{r}_{\mathrm{Rx}})$ which is computed as

$$\begin{aligned} G_{\mathrm{wb}}(\mathbf{r}_{\mathrm{Tx}}, \mathbf{r}_{\mathrm{Rx}}) = G_d(d) + G_{\mathrm{LS}}(\mathbf{r}_{\mathrm{Tx}}, \mathbf{r}_{\mathrm{Rx}}) \\ + \frac{1}{m} \sum_{i=1}^{m} 10 \log_{10} |Y_i(\mathbf{r}_{\mathrm{Tx}}, \mathbf{r}_{\mathrm{Rx}})|^2 \quad [dB] \end{aligned} \tag{3.7}$$

where $G_d(d)$ is the distance-dependent path-gain according to equation (3.1), $G_{\mathrm{LS}}(\mathbf{r}_{\mathrm{Tx}}, \mathbf{r}_{\mathrm{Rx}})$ the large scale fading process given by equation (3.2), m the diversity order of the channel from equation (3.5), and $Y_i(\mathbf{r}_{\mathrm{Tx}}, \mathbf{r}_{\mathrm{Rx}})$ the small scale fading process for sub-channel i from equation (3.6).

4 Analyzed Environments Types

Three different terrain types are considered in the performance evaluation of MPR-based broadcast, a flat rural area, a hilly rural area, and a urban area. To model the radio channel in the studied areas we use two different channel models. For the urban area we use the channel model introduced in Chapter 3. For the rural areas we use path-gain calculations from the propagation library DetVag-90® [13] to model the large-scale behavior of the radio channel. To model the small-scale behavior of the radio channel we use a small-scale fading model with the same model structure as the one used for urban scenarios.

4.1 Channel parameters for rural areas

The behavior of the urban channel models depends on the used parameter set while the behavior of the path-gain calculated with DetVag-90® [13] depends on the where on the map the network is placed. Thus, before we specific the channel parameters and terrain areas we use in the evaluation we estimate some large scale statistical parameters for different rural terrains types.

The large scale statistical parameters we estimate for different environment types are the constants in the distance dependent path-gain model, i.e. G_0 and n in equation 3.1, the standard deviation, σ_{LS}, of the large scale fading process, and the the large scale channel correlation, $(\Delta d)_{\mathrm{LS}}$, estimated by the autocorrelation function.

Estimation method

The parameters for the rural environments are estimated on calculated path-gain values for links in mobile scenarios in different terrains types. The used mobile scenarios consists of 64 nodes moving around for 3600 seconds in a square area of 256 km ^{2}. To model the movements of the nodes we use the random walk model used in [14]. To calculate the path-gain we use a uniform geometrical theory of diffraction (UTD) model by Holm [15, 16, 17] in the propagation library DetVag-90® [13].

The UTD model models the distance dependent path-gain and the large scale fading of the channel with high accuracy in rural areas. However, the effects of the small scale fading will not be modeled by the model. Thus only the parameters for the distance dependent path gain and large scale process can be extracted from the path gain calculations with the model. To model the terrain profile, we use a digital terrain database with a resolution of 50 m. All links in the scenarios is calculated once per second. For each link we thus get at time series of path-gain values.

The parameters in the distance dependent path-gain model are estimated in logarithmic scale as a least mean square problem. To estimate the parameters for the large scale fading process we first remove the distance dependent path-gain from the calculated values. We then estimate the autocorrelation function for each link in the

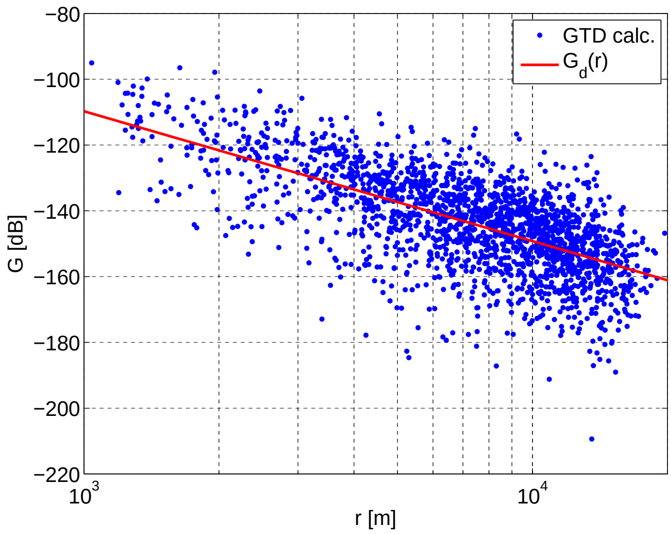

Figure 4.1: Subset of the calculated path-gains and the estimated distance dependent path-gain $G_d(r)$ as a function of of the distance, r, between the nodes in the Mantorp area.

scenario. The autocorrelation function for a certain environment is then calculated as the an average of the autocorrelation function for the individual links.

Results

We estimate large scale parameters for five different terrain types. The first, and easiest environment in terms of radio communication is a flat plain around Mantorp in Östergötland. The second environment around Veberöd in Skåne is also relative flat. The third environment is a rather hilly area with forests around Lomben in Norrbotten. Thereafter, an even more hilly area with forests around Bräcke in Jämtland is considered. As a worst case, we have also investigated a mountainous area in Lappland (north part of Sweden) around the mountain Kebnekaise.

A random subset of the calculated path-gains and the estimated distance dependent path-gain, $G_d(d)$, are presented in Figure 4.1 - 4.5. All estimated parameters for the large scale fading process are presented in Table 4.1.

If we compare Figure 4.1 and Figure 4.2 we can see that parameters for the distance dependent path-gain are relatively similar for the both flat terrain areas. Furthermore, we can see that the spread of the calculated path-gain values relative to the estimated distance dependent path-gain, $G_d(d)$, is slightly larger for the area around Veberöd in Figure 4.2. This is reflected in a larger σ_{LS} for the Veberöd arena compared to the Mantorp area in Table 4.1. In the table we can also see that the correlation of the large-scale fading process, $(\Delta d)_{\mathrm{LS}}$, is higher for the relatively flat Veberöd area than the very flat Mantorp area.

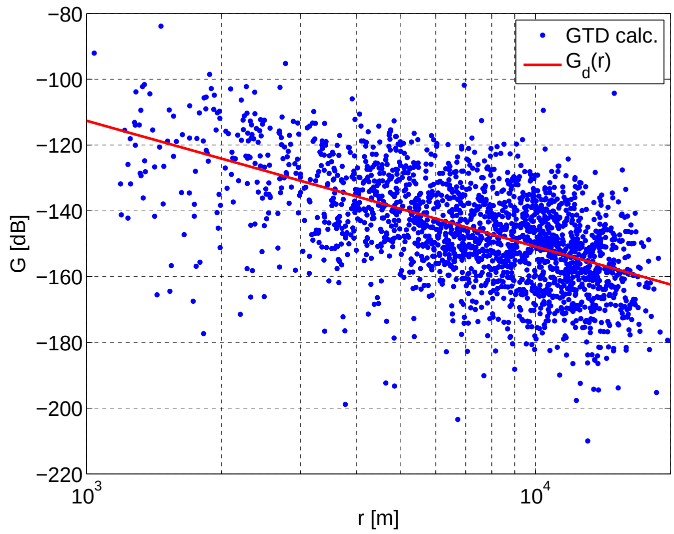

Figure 4.2: Subset of the calculated path-gains and the estimated distance dependent path-gain $G_d(r)$ as a function of of the distance, r, between the nodes in the Veberöd area.

If we compare Figure 4.3 and Figure 4.4 we can see that parameters for the distance dependent path-gain are relatively similar for the both hilly terrain areas. However, the difference in the spread of the calculated path-gain values relative to the estimated distance dependent path-gain, $G_d(d)$, is larger for the area around Bräcke in Figure 4.2. If we compare the estimated large-scale parameters in Table 4.1 can also see that the correlation of the large-scale fading process, $(\Delta d)_{\text{LS}}$, is higher for the Bräcke area than the Lomben area.

If we study Figure 4.5 with the results for the area around Kebnekaise we can see that slope of the distance dependent path-gain $G_d(d)$ is significantly higher than for the four other areas. This is also reflected in a higher path-gain exponent n in Table 4.1 for the Kebnekaise area. The spread of the calculated path-gain values relative to the distance dependent path-gain, $G_d(d)$, is also significantly higher in Figure 4.5 compared to the other areas. Furthermore, the correlation of the large-scale fading process, $(\Delta d)_{\text{LS}}$, is higher for this area.

The results in Table 4.1 shows that both the standard deviations, σ_{LS}, and correlation distance, $(\Delta d)_{\text{LS}}$ increases when the altitude variation in the studied areas increases. This indicates that the large variations of the large-scale fading process introduced by hills and mountains will vary relatively slow. However, even if the largest variations introduced by the large scale fading process happens relatively slow in rural areas it will still exist smaller and faster variations due to more fine-scale variations in the terrain. How this affect MPR-based broadcast will be further analyzed in Chapter 6.

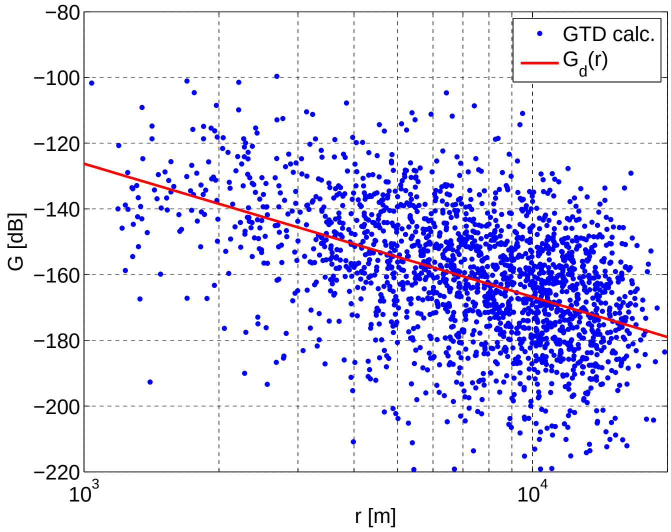

Figure 4.3: Subset of the calculated path-gains and the estimated distance dependent path-gain $G_d(r)$ as a function of of the distance, r, between the nodes in the Lomben area.

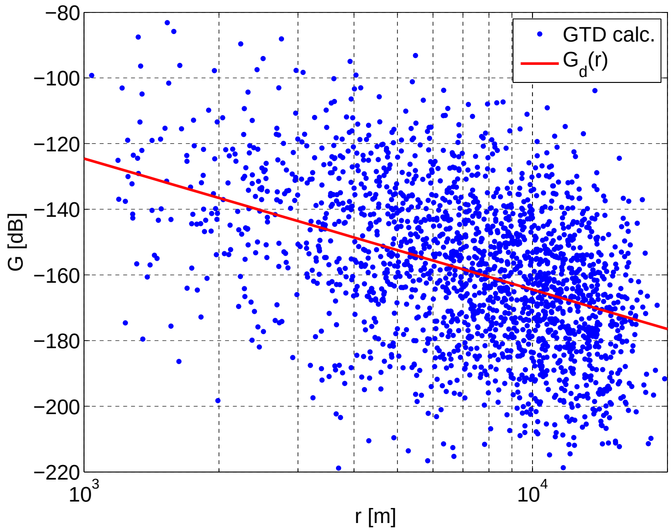

Figure 4.4: Subset of the calculated path-gains and the estimated distance dependent path-gain $G_d(r)$ as a function of of the distance, r, between the nodes in the Bräcke area.

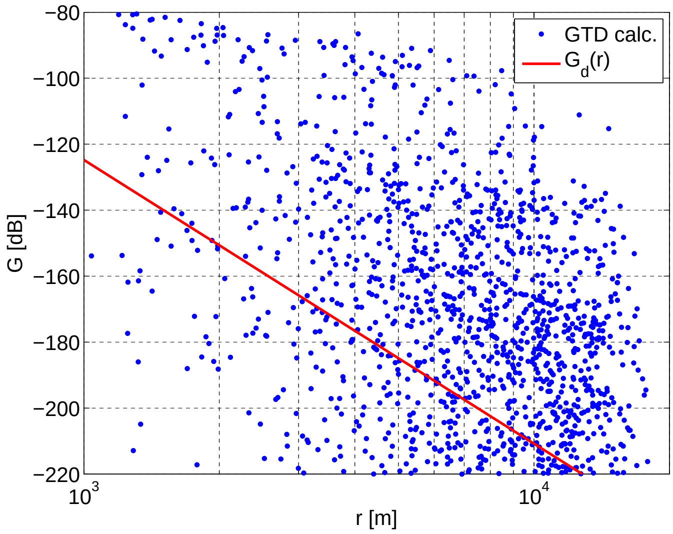

Figure 4.5: Subset of the calculated path-gains and the estimated distance dependent path-gain $G_d(r)$ as a function of of the distance, r, between the nodes in the Kebnekaise area.

Area	G_0 [dB]	n [-]	σ_{LS} [dB]	$(\Delta d)_{\mathrm{LS}}$ [m]
Manttorp	-110	3.95	4.66	666
Veberöd	-113	3.82	5.24	815
Lomben	-126	4.05	6.40	1050
Bräcke	-124	3.99	7.44	1180
8 Kebnekaise	-125	8.60	18.2	2430

Table 4.1: Large scale parameters estimated on the calculated path-gains for different areas.

Type	Area	Description
Urban	City of Linköping	Small town
Flat rural	Area around Mantorp	Flat plain
Hilly rural	Area around Bräcke	Hilly area with forests

Table 4.2: Terrain types used in network simulations.

Model	G_0 [dB]	n [m]	$\sigma_{\bar{G}_{\mathrm{LS}}}$ [dB]	$(\Delta d)_{\bar{G}_{\mathrm{LS}}}$ [m]	$\sigma_{\widetilde{G}_{\mathrm{LS}}}$	$(\Delta d)_{\widetilde{G}_{\mathrm{LS}}}$
Urban	-128	3.93	6.6	200	3.1	20
Urban no blocks	-128	3.93	-	-	3.1	20
Plane Earth	-128	3.93	-	-	-	-

Table 4.3: Large scale parameters used for different terrain types.

4.2 Evaluated environments

In the evaluation of MPR-based broadcast three environment types are evaluated, a flat rural area, a hilly rural area, and a city area, see Table 4.2. The flat rural area is based on the flat plain around Mantorp, previously used in Section 4.1. The hilly rural area is based on the Bräcke area, also used in Section 4.1. The city area is based on the city of Linköping which was used as reference when developing the city channel model, [12].

To model the large scale variations of the path-gain for the two rural terrain ares we use the same model as in Section 4.1, i.e. a uniform geometrical theory of diffraction (UTD) model by Holm [15, 16, 17]. To model the small scale variations of the path-gain we reuse the model for small scale fading that was presented in Section 3.3.

To model the path-gain for the urban scenario we use the channel model presented in Chapter 3. All parameters in the model is based on the same measurements in the city of Linköping as the parameters for the original non reduced channel model in [12]. However, the values of some of the parameters are not the same because of a minor adjustment of the used receiver routes.

The parameters used for the urban area is presented in Table 4.3. Two different versions of the urban model are evaluated. The first, denoted with *Urban* utilize the full model. The second version, denoted with *Urban no blocks*, ignores the $\bar{G}_{\mathrm{LS}}$ part of the model, i.e. we do not model the effects of the blocks in the city.

As a reference model we also use a model that only model the distance dependent part of the path-gain. This model is denoted as the *Plane earth* model. The used parameters for this model is also presented in Table 4.3.

Two different parameter sets is used for the small scale fading process, see Table 4.4. The first parameter set represent a channel with limited diversity. The parameters

Area	W_{coh} [MHz]	K [-]	$(\Delta d)_{SS}$ [m]
Default	1.16	0.796	6.67
Wide Band (WB)	-	-	-

Table 4.4: Small scale parameters used for different terrain types.

used for this channel is based on the measurements in Linköping, [12]. The second parameter set represents a channel with high diversity. The first parameter set is the default set for all three environments in Table 4.2. When the second high diversity channel is used we add the suffix *WB*, i.e. Wide Band, to the terrain type, for example Flat WB.

5 System and Simulation Setup

To evaluate the MPR selection methods we use an in house radio network simulator. The simulator is written C++ and models the system at packet level.

5.1 Physical Model

It is essential to capture the channel effects of a highly dynamic mobile scenario. To accomplish that the stochastic channel model for simulations of mobile ad hoc networks described in Chapter 3 is employed. It captures the essence of the channel characteristics, and copes with the constraint of low computational complexity.

The receiver chain needs to decide whether a packet can be correctly received. Based on the channel realization when the packet is sent an instantaneous channel capacity is computed and used for the packet decision. If the data rate of the packet is larger than, or at most equal to, this channel capacity the packet is either declared erroneous or correctly received. Notice, however, that no system will reach the channel capacity, there will always be some implementation losses, but we ignore such losses here. It is the channel dynamics fluctuations that are our main focus here

The performance of modern advanced systems depends mainly on the instantaneous SNR, averaged over the system bandwidth. Thus, the average SNR over the packet and its bandwidth is calculated as physical layer information for the routing decisions.

5.2 MAC-Layer

A basic TDMA MAC protocol is used for the evaluation. The time is divided into time slots, which are grouped into repeating frames. Each node has a time slot in each frame and the traffic in the network is kept sufficiently low to avoid congestion in the network. In our evaluation the MAC protocol can support a total data rate of 751.6 kbps, i.e. approximately 11.7 kbps per node. A time slot is 7.81 ms, containing 512 bits user data.

There are three reasons for selecting such a TDMA protocol. Firstly, no robustness issues have to be addressed at the MAC layer due to packet collisions. This would be the case if a random access protocol is used. Secondly, network throughputs and capacities can be computed analytically. Thirdly, many military networks use TDMA-based MAC protocols. Nevertheless, the focus of this paper is not on the MAC layer, or scheduling, but on the broadcast performance.

5.3 Scenario

Different environments are considered but for a given environment the scenario consists of 64 nodes moving around for 400 seconds in a square area of 64 km ^{2} at a speed of 50 km/h. To model the movement of the nodes we use the random walk model used in [14]. All nodes moves independent of each other, and if a node hits the boundary of the square, it will reflect back like a ball. As connectivity in the network is important for the results, we investigate networks of different connectivity, from sparse to very dense network. To obtain different network connectivities we adjust the output power of the nodes in then the scenario. As a measure of the networks connectivity we use the average number of neighbors the nodes have detected, which we denote with N_e.

5.4 Traffic

Both user and overhead traffic are sent in the network. However, a rather simple user traffic model is employed since the user traffic is only used to probe the network and generate performance measurements. The user traffic is modeled as broadcast transmissions of packets. A source sending one packet is randomly selected among the 64 nodes. Thereafter, a new source is randomly selected and so on. We transmit an average of 64 user packets per second. The traffic load in the network is sufficiently low to prevent packet queues from building up in the nodes. However, a sent packet may not reach one of its intended receiving node if the link to that node has disappeared. If this happens the packet may not reach all its destinations and if not all destinations are reached the delivery ratio is reduced.

5.5 Measurements

The performance is measured in terms of delivery ratio, and the cost in terms of retransmissions and HELLO message overhead. As a measure of how well the network is connected we use the number of neighbors any given node has in average, denoted N_e. For each packet a node A sends, the number of nodes that are able to receive the packet, measured at MAC-layer, is the number of neighbors to the node A at that time. The average value N_e is then obtained by in this way considering all the transmissions from all the nodes during one simulation run.

Delivery Ratio (η):

The percentage of packets that reach the destinations. A packet not reaching the destination is lost either because no route exists, or that a link deteriorates so that a transmitted packet cannot be received. No acknowledgments or ARQ mechanisms are used on the link level, i.e., between a transmitter and a given receiver.

Network Capacity (C):

The capacity left for the users in the network to send their user data after the capacity for the overhead traffic is deducted. We estimate the network capacity as

$$C = \frac{R_{sys} - R_{\text{HELLO}}}{N_{\text{trans}}\ R_{sys}} \tag{5.1}$$

where R_{sys} is the data rate the MAC layer can deliver to the upper layer, R_{HELLO} is the average data rate used by the HELLO messages, and N_{trans} is the average number of transmissions of a user messages that occurs. For example, assume a connected network of $N = 64$ nodes. If full flooding is used $N_{\text{trans}} = 64$ while $R_{\text{HELLO}} = 0$ and we get a capacity $C = 1/64 = 0.016$. If we have a single hop network, i.e. all nodes have all 63 other nodes as neighbors, and use an effective MPR-based multicast algorithm, only one transmission is necessary. However, HELLO messages require some resources, so C will not be 1 but close to 1. Finally, when we talk about the cost of a method we mean $1 - C$.

6 Results - different environments

We are interested in how the different statistical channel parameters influence the performance. To investigate this we only consider MPR-default and show how the performance is affected by changing different parameters in the channel model for the urban environment.

As a start we are interested in what fading margins that are needed to overcome the fast fading on a link. In Figure 6.1 the required fading margin γ to obtain a packet error rate of at most one percent is examined in the case of small scale fading. This margin depends on the number of independent channels, or diversity and the Ricean-K factor on these channels. For a Reyleigh channel ($K = 0$), a fading margin of 20 dB is required, but by increasing the diversity order to two, or four a fading margin of 11 and 7 dB is sufficient, respectively.

In Figure 6.2 we study the packet delivery ratio η of the MPR-default method for different large scale fading parameters. The small scale fading is ignored. The two parameters considered is the large scale correlation distance $(\Delta d)_{G_{\mathrm{LS}}}$ and the standard deviation of the large scale fading $\sigma_{G_{\mathrm{LS}}}$. As can be seen, the correlation distance starts to be rather important for the packet delivery ratio when the variance increases. At a point when the correlation distance is about 100 m the curves start to ascend and η to increase. However, the location of this point is dependent on the mobility (here 50 km/h) and the HELLO message re-transmission interval (here 2 seconds). By either reducing the speed, or the re-transmission interval this point is moved leftwards. This means that a smaller correlation distance is manageable. Table 4.1 and 4.3 present values on the correlation distance $(\Delta d)_{G_{\mathrm{LS}}}$ and standard deviation $\sigma_{G_{\mathrm{LS}}}$ for different terrains. Values between three and eight are realistic for the standard deviation, except when mountainous terrains like Kebnekaise is considered. The correlation distance is smallest for urban environments when 200 meter, or even smaller distances are typical, but the other environments have considerably larger correlation distances.

How the the MPR-default method performs for different environments is examined in Figure 6.3 and Figure 6.4. The environments are those presented in Chapter 4; Flat rural, Flat rural WB, etc. Note that on the x-axis we use the path loss the system can overcome. That is, the highest path loss the system can handle and receive packets correctly. We call it the manageable path loss. The main conclusion from these figures is that the environment has a large impact on the performance. In Figure 6.3 the average number of neighbors for the different environments are shown. For the flat rural terrain the networks get connected first, i.e., the system needs to overcome the smallest average path losses. In Figure 6.4 we can see that it is first when the path loss the system can overcome reaches about 140 dB a reasonably acceptable deliver ratio can be obtained. The networks are either fragmented or too sparsely connected for lower values on that path loss. It is for the flat rural (or plane earth) the MPR-deafult works best. Then a good and reliable delivery ratio is obtained when the manageable path loss reaches about 160 dB. For the urban terrain there is a drop in delivery ratio at a manageable path loss of about 160 dB, and a manageable path loss of almost 170 dB is needed for it to work satisfactory. For the hilly terrain it is first when the manageable path loss reaches above 180 dB a good delivery ratio is achieved. We can see that the

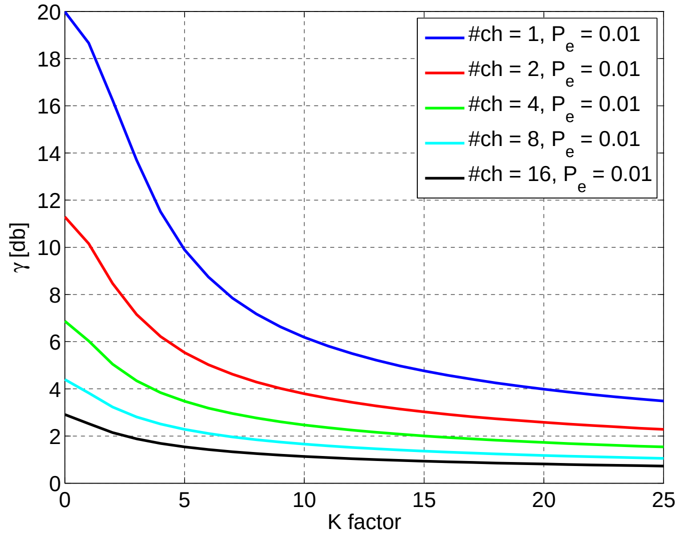

Figure 6.1: Rice fading: The required fading margin γ to obtain at most one percent packet error rate for different number of channels and K factors.

MPR-default requires a very high manageable path loss for the urban and and hilly terrains to be robust. Moreover, there are difference between the results using the default model for the environment types and the corresponding wide band models. However, using a wide band, instead of narrow band system, does not solve the problem with insufficient robustness.

The shapes of the curves in Figure 6.4 depend on the terrain. In the urban case, the delivery ratio drops to a low value for a path loss of about 160 dB. This is because the number of MPRs selected is low. On the other hand, for a path loss of about 145 dB a good delivery ratio is obtained. A large scale fading variance makes sufficient number of links good enough for communication, and MPR default is forced to select many nodes as MPRs. In the flat rural terrain the deliver radio is gradual increased. For a large part of the network a good connectivity can be obtained for a small manageable path loss, but at this small path loss some part of the nodes still have a poor connectivity. It is first at a considerably larger manageable path loss the whole network gets a good connectivity. In the hilly rural terrain a high manageable path loss is required to obtain a good delivery ratio. Then the network is well connected, but for a smaller manageable path loss too few MPRs are selected. At a manageable path loss of 145 dB only about 3.5 MPRs are selected by each node in average in the hilly terrain, but as many as about 6 MPRs in the urban terrain. As a consequence, the delivery ratio is almost 0.98 in the urban terrain but only 0.91 in the hilly terrain.

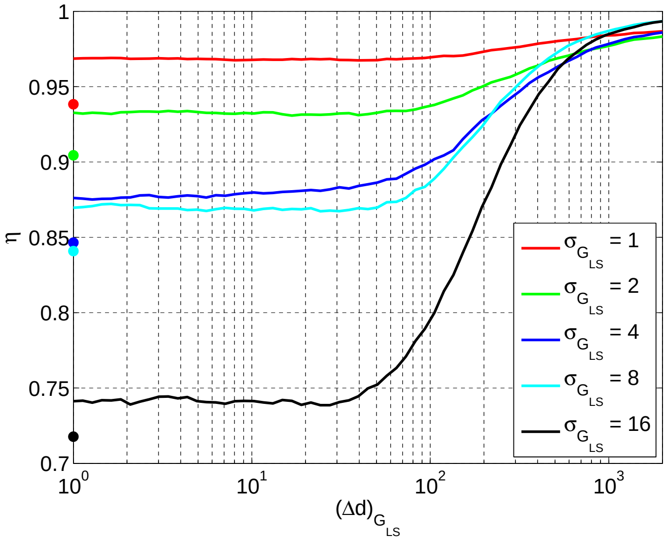

Figure 6.2: Packet delivery ratio η for the MPR-default method for different large scale fading parameters.

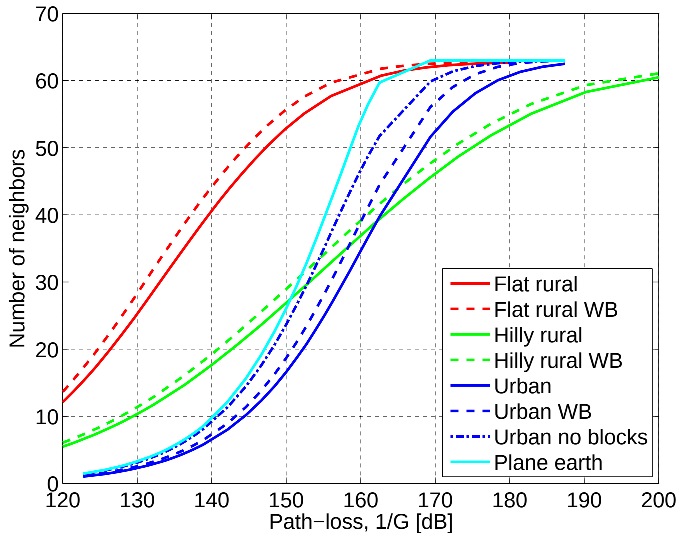

Figure 6.3: Number of neighbors for different environments.

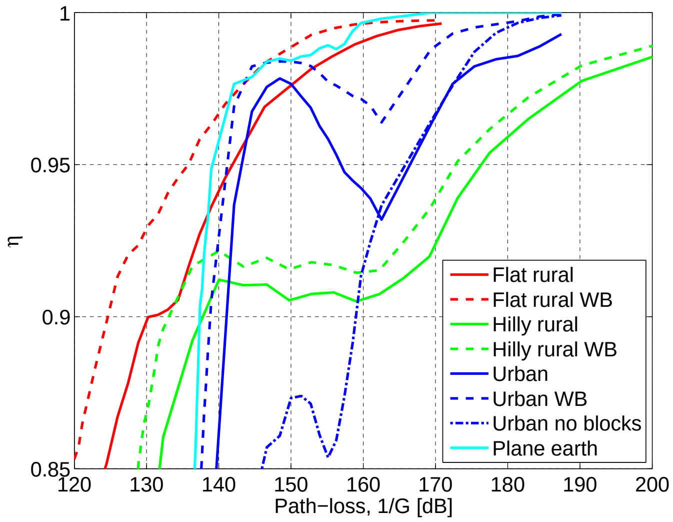

Figure 6.4: Packet delivery ratio η for the MPR-default method for different environments.

7 Results - different methods

We are interested in robust flooding, i.e. the delivery ratio should be high, over 95 percent. In all the figures the results, delivery ratio and network capacity, are plotted against the network connectivity, measured as the average number of neighbors N_e, on the x-axis. As a reference, the results for full flooding and for the MPR-default method with a retransmission interval of 2 seconds are included in all figures. Note that the networks are fragmented for small values on N_e. It is only when N_e is around 10 that the networks gets connected and full flooding reaches a delivery ratio of 1. However, the required N_e for the networks to get connected varies slightly between the different environments.

7.1 Flat rural area

In Figures 7.1 and 7.2 the delivery ratio for the different methods in a flat rural area is shown. The capacities for the methods are displayed in Figure 7.3 and 7.4.

Fading/SNR Margin

The delivery ratio for different types of fading margins are plotted in Figures 7.1. The standard MPR hysteresis method is denoted *MPR-link hyst. basic*. A fading margin of 4 and 16 is used in the *MPR-phy.info. SNR,* $\gamma_m = \{4, 16\}$, respectively. In the method denoted *MPR-phys.info. SNR,* $\gamma_m = 1$ no fading margin is used. However, lower layer information is utilized to decide on which links to remove, that is, a bad link can be removed more quickly from the list of usable links by using lower layer information. By doing this, a considerably better delivery ratio is obtained compared with MPR-default. We can note that the standard MPR hysteresis method has a good delivery ratio despite that no physical layer information is used. However, it is beneficial to use physical layer information and a fading margin. Selecting the small margin of 4 dB, or no margin at all, is much better for most connectivities, in particular for sparse networks. However, the higher margin of 16 dB is slightly better for dense networks. Note that with a fading margin the number of links that are used is reduced. For very sparse networks, it is important to be able to use all possible links, even if they are poor, because it makes the network better connected, which also increases the delivery ratio.

Additional MPRs and MPR Relay Assistance

The delivery ratio for methods that choose additional MPRs and for the MPR relay assistance method are plotted in Figure 7.2. The notations *MPR-coverage* $= \{2, 4, 8\}$ are used for the methods selecting two times, four times, and eight times as many

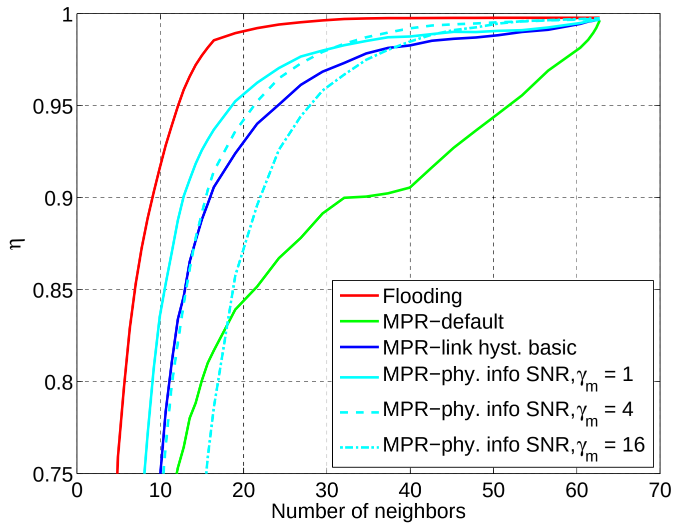

Figure 7.1: Delivery ratio when using fading margins for a flat rural area.

MPR nodes as the MPR-default method, respectively. When four times as many MPRs are selected a high deliver ratio is achieved and no drop in delivery ratio for certain values on N_e occurs. Selecting eighth times as many MPRs only gives a negligible additional improvement at a high cost. On the other hand, only selecting two times as many MPRs may be a compromise when also considering the network capacity. As can be seen, the MPR relay assistance method has a competitive delivery ratio when considering that the cost is lower than for the method that uses four additional MPRs. For sparse networks the MPR relay assistance method is better than the method that selects four additional MPRs, but when the networks get dense the latter method starts to display a slightly better delivery ratio.

7.2 Hilly rural area

In Figures 7.5 and 7.6 the delivery ratio for the different methods in a hilly rural area is shown. The capacities for the methods are displayed in Figure 7.7 and 7.8.

Fading/SNR Margin

The delivery ratio for different types of fading margins are plotted in Figure 7.5. We can note that the standard MPR hysteresis method has a good delivery ratio despite that no physical layer information is used. However, it is beneficial to use physical layer

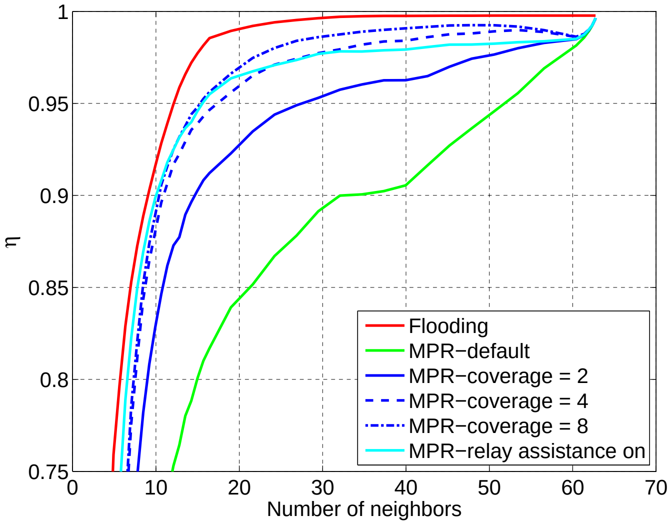

Figure 7.2: Delivery ratio for methods selecting different number on MPRs and the hybrid method for a flat rural area.

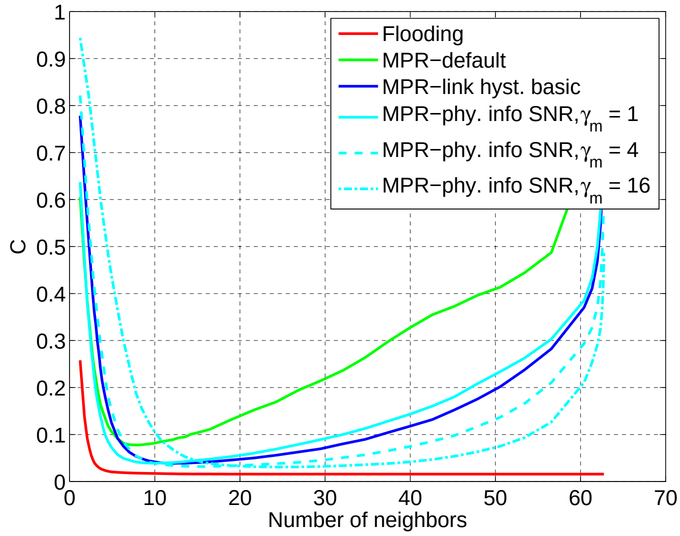

Figure 7.3: Network capacity when using fading margins for a flat rural area.

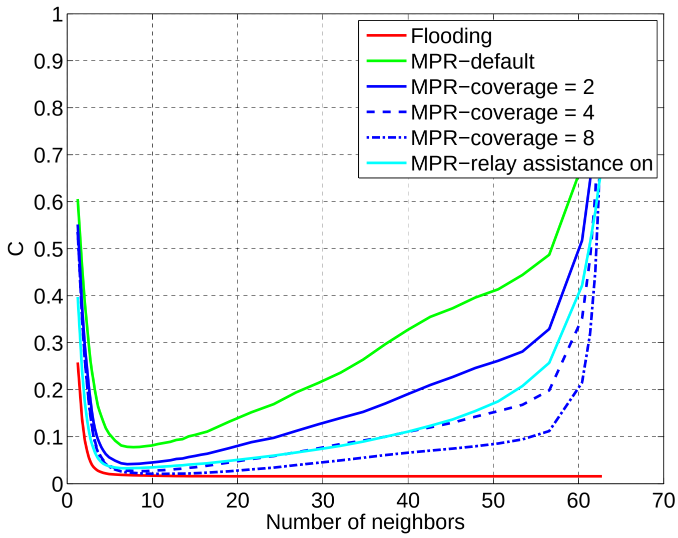

Figure 7.4: Network capacity for methods selecting different number on MPRs and the hybrid method for a flat rural area.

information, but for sparse networks a small fading margin, or no margin at all should be used. It can be seen that the method with a fading margin of 16 dB does not work so well for sparse networks, but starts to display a slightly better delivery ratio for dense network compared to the methods with a smaller fading margin. Moreover, for a hilly urban area the MPR-default method does not provide a satisfactory delivery ratio.

Additional MPRs and MPR Relay Assistance

The delivery ratio for methods that choose additional MPRs and for the MPR relay assistance method are plotted in Figure 7.6. As for the flat rural area, when four times as many MPRs are selected a high deliver ratio is achieved and no drop in delivery ratio for any given values on N_e occurs. When also the cost is considered, the MPR relay assistance method may be an option though. When comparing to methods using fading margins, the methods choosing additional MPRs are slightly better for sparse networks.

7.3 Urban area

In Figures 7.9 and 7.10 the delivery ratio for the different methods in an urban area is shown. The capacities for the methods are displayed in Figure 7.11 and 7.12.

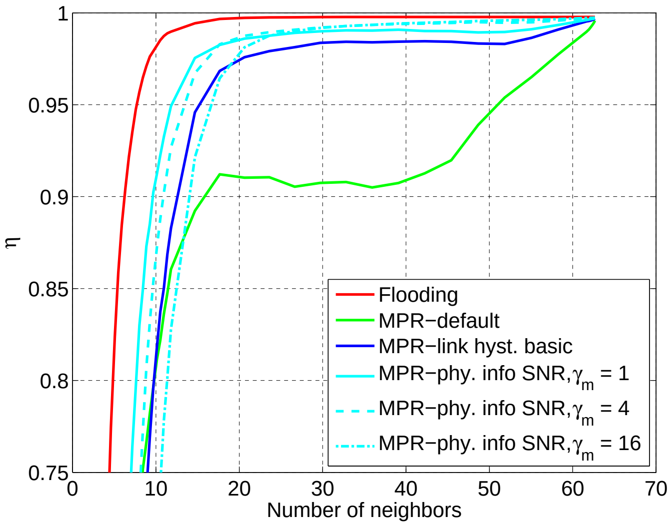

Figure 7.5: Delivery ratio when using fading margins for a hilly rural area.

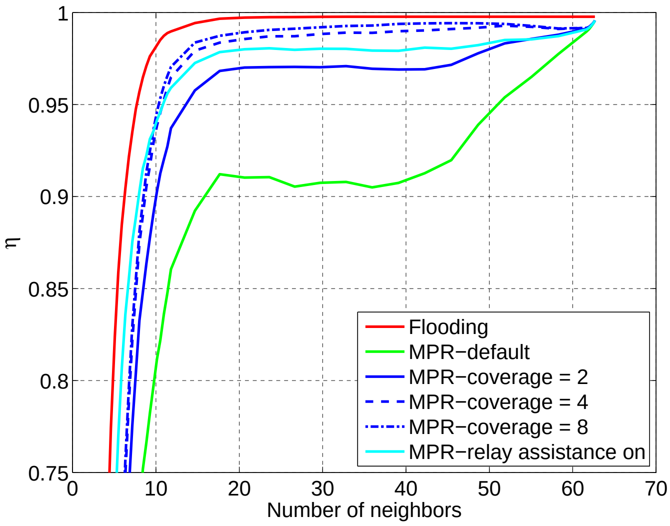

Figure 7.6: Delivery ratio for methods selecting different number on MPRs and the hybrid method for a hilly rural area.

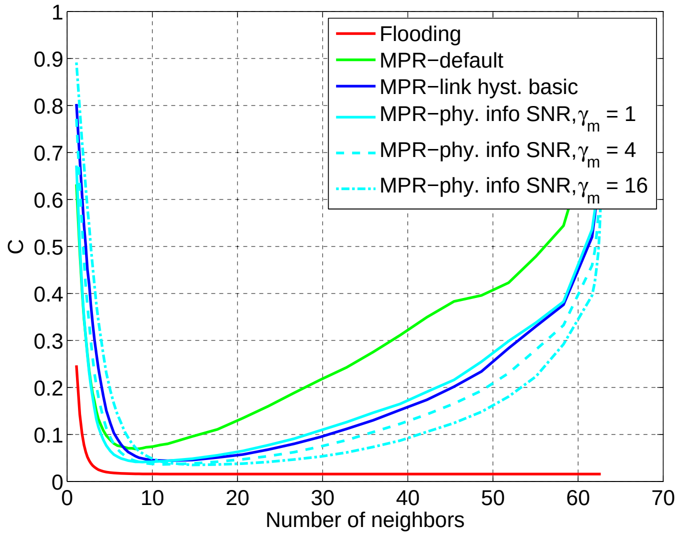

Figure 7.7: Network capacity when using fading margins for a hilly rural area.

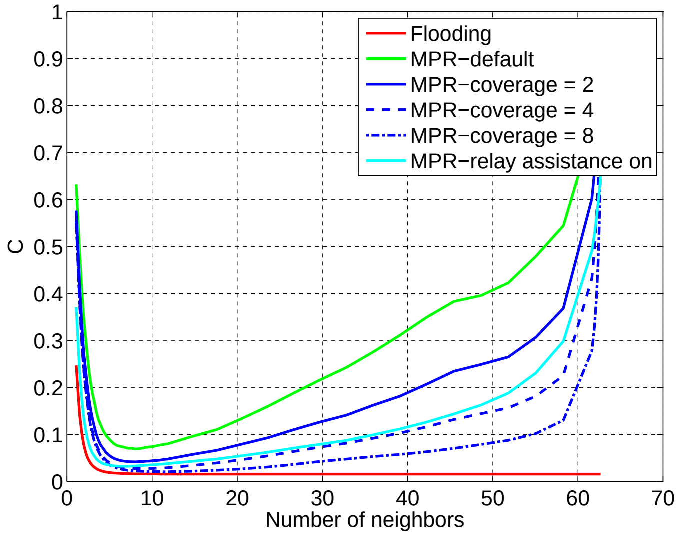

Figure 7.8: Network capacity for methods selecting different number on MPRs and the hybrid method for a hilly rural area.

Fading/SNR Margin

The delivery ratio for different types of fading margins are plotted in Figure 7.9. The MPR-default has a good delivery ratio for sparse networks, but when the number of neighbors increase the delivery ratio starts to decrease until it reaches its lowest levels for about 40 number of neighbors. For these network types, the number of redundant MPRs selected is low, i.e., low probability of having an alternative route when a link disappears. Either the probability that a link disappears has to be reduced which can be accomplished by only using reliable links, or more MPRs can be selected so backup routes exists. Among the methods using fading margins, their behavior is similar to as they behaved in the the other environments. However, what become even more evident in the urban terrain is that the method using a fading margin of 16 dB suffers when the networks are sparse. For dense networks, on the other hand, it again displays a slightly better delivery ratio than the methods with a smaller fading margin.

Additional MPRs and MPR Relay Assistance

The delivery ratio for methods that choose additional MPRs and for the MPR relay assistance method are plotted in Figure 7.10. In this case, the method selecting two times as many MPRs has a drop in delivery ration for about 40 number of neighbors. As for MPR-default, the reason is that the probability of having an alternative route when a link disappears is not high enough so more additional MPRs are needed. In the urban terrain the MPR relay assistance method has the best delivery ratio unless the networks are dense, close to that of full flooding, and the cost is lower than for the method that uses four additional MPRs. However, for the dense networks the method selecting four times as many MPRs is only slightly better than the MPR relay assistance method.

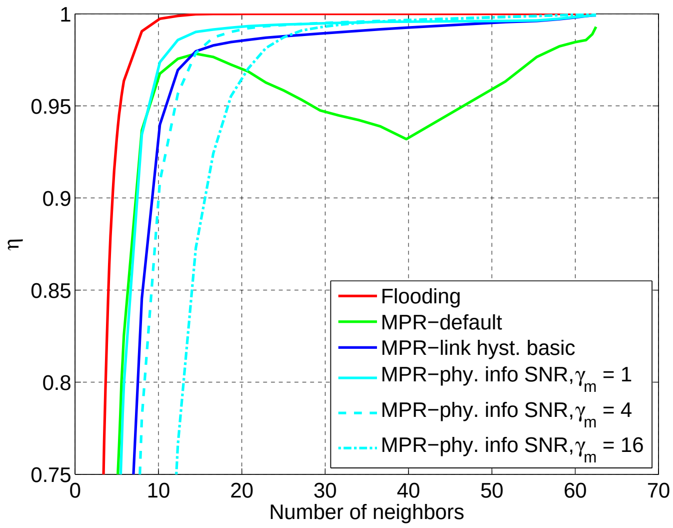

Figure 7.9: Delivery ratio when using fading margins for an urban area.

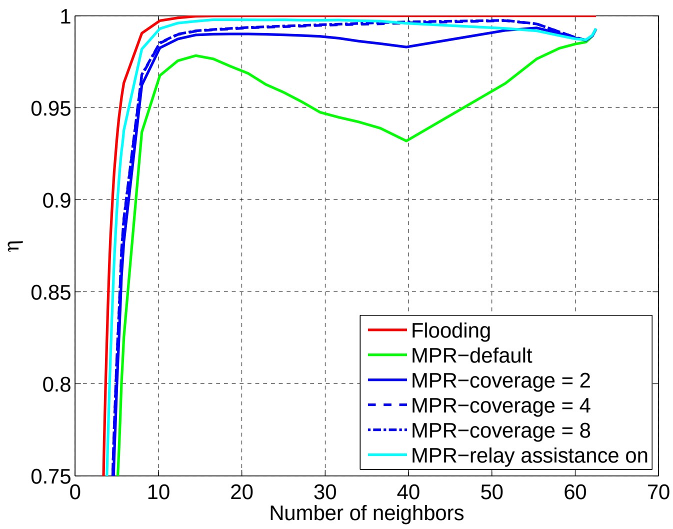

Figure 7.10: Delivery ratio for methods selecting different number on MPRs and the hybrid method for an urban area.

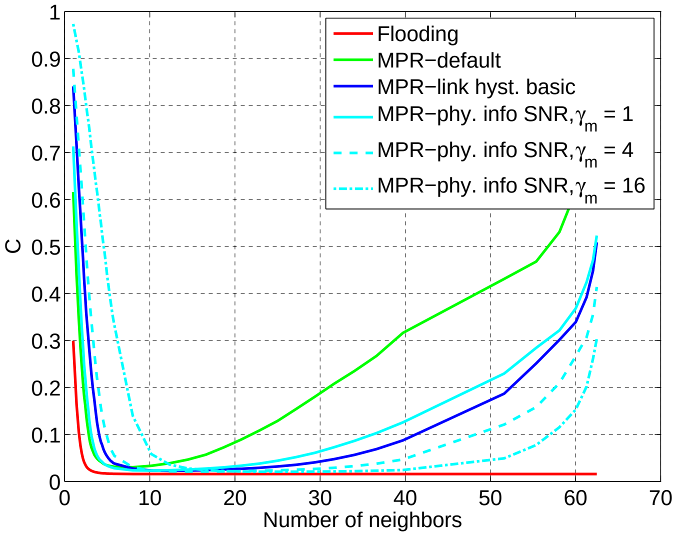

Figure 7.11: Network capacity when using fading margins for an urban area.

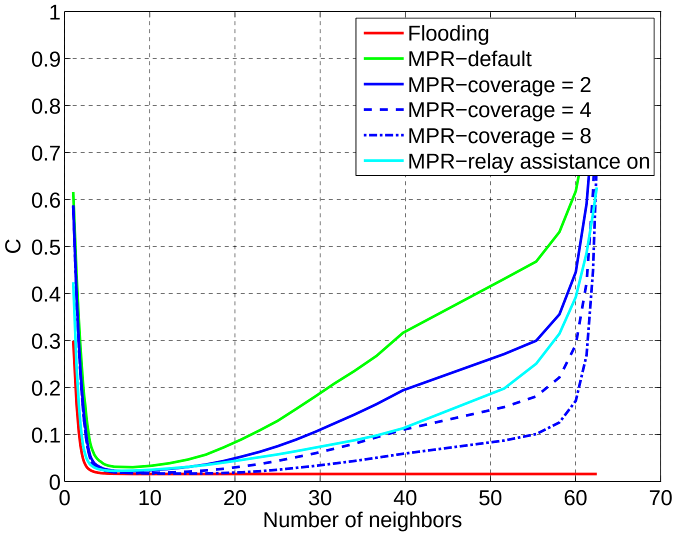

Figure 7.12: Network capacity for methods selecting different number on MPRs and the hybrid method for an urban area.

8 Discussions

In this chapter we first discuss some principles of the MPR selection process in mobile scenarios, and thereafter how the terrain and network connectivity affects the performance.

We investigated as an option a probabilistic method that tried to use probabilities in the selection of suitable MPRs. Note that the MPRs need to be selected so that all two-hop neighbors are reached. However, which nodes and how many nodes that are selected as MPRs can still vary. The basic idea was to estimate the probability that a given two-hop neighbor is reached. This probability can be derived from the physical layer information. Then in the selection process we set a threshold probability, and select the MPR nodes so that all the two-hop neighbors are reached with this probability if possible. This means e.g., that in some cases several paths to a given two-hop neighbor are needed to satisfy this threshold probability.

However, this optional method do not work as well as expected. The main deficiency is that only the two-hop neighborhood is considered. However, a two-hop neighbor can also be reached by three hops. Therefore, all paths, not only the two-hop paths to a given node should be considered. This is because also paths longer than two-hop have a non negligible contribution to the probability of reaching a given node. On the other hand, to gather information further away then from the next-hop node, takes too much time so the estimates will probably not be accurate enough. Also, the HELLO messages does not support such gathering so additional control messages, or the TC messages, are needed. As a consequence we concluded that such a probabilistic method is not efficient in mobile scenarios. Trying to estimate by probabilistic methods which MPR nodes to select does not give good enough results. In fact, the method that selects some additional MPRs to obtain some network diversity work as well as the probabilistic method.

The environment can have a large affect on the performance of a given method. On the other hand, the mutual ranking between the different methods is not so much affected by the environment. There are some minor influences on the mutual ranking but they are not significant, e.g., a method that is robust in an urban terrain is also robust in an hilly terrain, and then also in a flat terrain. The flat rural terrain is easiest to deal with, and in this terrain also MPR-default works reasonable well. For the other terrains MPR-default is not robust enough. Using physical information and a fading margin is beneficial, however, what size to chose on this margin depends on how well the network is connected. As long the network is well connected, a fairly large margin can be used. In fact, for a very dense network a fading margin of 16 dB worked best, but only slightly better than using the smaller margins. However, for sparse networks a large margin is not a good choice, in that case a small margin or no margin at all should be used. In such cases, it is important to consider and use all possible links so a good enough connectivity can be achieved. A fading margin means that marginal/weak links are not used. Adapting margins after connectivity would be difficult. Therefore, as the gains only are small for dense networks with a large fading margin, the conclusion is that the margin should be small, not larger than 4 dB.

Finally, a summery of the results in the figures of the previous chapter for $N_e =$

	Number of neighbors			
	16	48	16	48
	η		C	
Flodding	0.983	0.998	0.016	0.016
MPR-default	0.813	0.937	0.109	0.397
MPR-link. hyst. basic	0.900	0.987	0.041	0.177
MPR-link. hyst. SNR, $\gamma_m = 1$	0.934	0.990	0.047	0.209
MPR-link. hyst. SNR, $\gamma_m = 2$	0.908	0.995	0.032	0.118
MPR-link. hyst. SNR, $\gamma_m = 16$	0.770	0.993	0.040	0.064
MPR-coverage = 2	0.910	0.974	0.063	0.247
MPR-coverage = 4	0.944	0.988	0.037	0.143
MPR-coverage = 8	0.954	0.993	0.023	0.080
MPR-relay assistance on	0.953	0.982	0.043	0.156

Table 8.1: Summary of the simulation results for a flat rural area.

$\{16, 48\}$ is presented in the Tables 8.1, 8.2, and 8.3.

	Number of neighbors			
	16	48	16	48
	η		C	
Flodding	0.995	0.998	0.016	0.016
MPR-default	0.901	0.935	0.102	0.393
MPR-link. hyst. basic	0.956	0.983	0.048	0.227
MPR-link. hyst. SNR, $\gamma_m = 1$	0.979	0.989	0.052	0.247
MPR-link. hyst. SNR, $\gamma_m = 2$	0.974	0.995	0.040	0.188
MPR-link. hyst. SNR, $\gamma_m = 16$	0.940	0.995	0.035	0.143
MPR-coverage = 2	0.962	0.977	0.061	0.246
MPR-coverage = 4	0.981	0.992	0.037	0.142
MPR-coverage = 8	0.985	0.994	0.023	0.077
MPR-relay assistance on	0.975	0.982	0.045	0.159

Table 8.2: Summary of the simulation results for a hilly rural area.

	Number of neighbors			
	16	48	16	48
	η		C	
Flodding	1.000	1.000	0.016	0.016
MPR-default	0.977	0.954	0.054	0.396
MPR-link. hyst. basic	0.982	0.995	0.024	0.156
MPR-link. hyst. SNR, $\gamma_m = 1$	0.991	0.996	0.027	0.198
MPR-link. hyst. SNR, $\gamma_m = 2$	0.985	0.998	0.021	0.098
MPR-link. hyst. SNR, $\gamma_m = 16$	0.910	0.998	0.025	0.042
MPR-coverage = 2	0.990	0.989	0.034	0.247
MPR-coverage = 4	0.992	0.997	0.023	0.143
MPR-coverage = 8	0.992	0.997	0.017	0.078
MPR-relay assistance on	0.998	0.994	0.034	0.172

Table 8.3: Summary of the simulation results for an urban area.

9 Conclusions

In a highly dynamic scenario the MPR-default method does not provide a satisfactory robustness, i.e., delivery ratio. The exception is for well connected networks in flat rural environments. Several methods, or combinations of methods can be used to increase the robustness. We investigate using physical layer information and a fading margin or additional MPRs. However, the cost of introducing these methods also needs to be considered.

The environment affects the performance of a given method, sometimes significantly. On the other hand, the mutual ranking between the different methods is not so much affected by the environment. Network connectivity, whether the network is sparse or dense, also has an impact on whether a choice is good or not. For sparse networks, using additional MPRs works best. However, for dense networks using a fading margin (or link hysteresis) is slightly better. Nevertheless, in a design only a small fading margin should be used to have a viable solution covering all network types, from sparse to dense networks.

References

[1] J. Macker. Simplified multicast forwarding (SMF). Internet-draft, IETF, Network Working Group, January 2012.

[2] T. Clausen and P. Jacquet. Optimized link state routing protocol(OLSR). RFC 3626, IETF, Network Working Group, October 2003.

[3] P. Jacquet, A. Laouiti, P. Minet, and L. Viennot. Performance analysis of OLSR multipoint relay flooding in two ad-hoc wireless network models. Technical report, INRIA, Reserach report 4260, September 2001.

[4] A. Busson, N. Minet, and E. Fleury. An analysis of the multipoint relays selection in OLSR. Technical report, INRIA, Reserach report 5468, January 2005.

[5] M. Benzaid, P. Minet, and K. Al Agha. Integrating fast mobility in the OLSR routing protocol. Technical report, INRIA, Reserach report 4510, June 2002.

[6] M. Benzaid, P. Minet, and K. Al Agha. Analysis and simulation of fast-OLSR. In *Vehicular Technology Conference, 2003. VTC 2003-Spring. The 57th IEEE Semiannual*, volume 3, pages 1788 – 1792 vol.3, april 2003.

[7] E. Larsen, L. Landmark, V. Pham, O. Kure, and P.E. Engelstad. Optimized group communications for tactical military networks. In *MILITARY COMMUNICATIONS CONFERENCE, 2010 - MILCOM 2010*, pages 1905 – 1911, Nov 2010.

[8] D. Yelemou, P. Mesure, and A-M. Poussard. A new BER-based approach to improve OLSR protocol. In *Wireless and Optical Communications Networks (WOCN), 2011 Eighth International Conference on*, May 2011.

[9] D. Gantsou and P. Sondi. Efficient selection of multipoint relays in wireless ad hoc networks with realistic physical layer. In Serge Fdida and Kazunori Sugiura, editors, *Sustainable Internet*, volume 4866 of *Lecture Notes in Computer Science*, pages 48–59. Springer Berlin / Heidelberg, 2007.

[10] F. Ingelrest and D. Simplot-Ryl. Maximizing the delivery of MPR broadcasting under realistic physical layer assumptions. *Journal Of Computer Science And Technology*, 23(3):451–460, 2008.

[11] J. Nilsson and U. Sterner. Robust MPR-based flooding in mobile ad-hoc networks. In *MILITARY COMMUNICATIONS CONFERENCE, 2012 - MILCOM 2012*, pages 1–6, 2012.

[12] G. Eriksson, K. Fors, and K. Wiklundh. A stochastic channel model for simulation of mobile ad-hoc networks. In *COST2100, TD(10)11084, Aalborg, Denmark*, June 2010.

[13] B. Asp, G. Eriksson, and P. Holm. Detvag-90® — Final Report. Scientific Report FOA-R–97-00566-504–SE, Defence Research Est., Div. of Command and Control Warfare Technology, Linköping, Sweden, September 1997.

[14] T. Holmberg, J. Grönkvist, J. Nilsson, and Mattias Sköld. Traffic estimation in mobile tdma-based ad hoc networks. In *The Sixth Annual Mediterranean Ad Hoc Networking WorkShop*, Corfu, Greece, June 12-15 2007.

[15] P. D. Holm. UTD-diffraction coefficients for higher order wedge diffracted fields. *IEEE Trans. Antennas Propagat.*, AP-44(6):879–888, June 1996.

[16] P. D. Holm. Higher order diffracted fields and multiple-edge transition zone diffraction. In *Proc. RVK99.*, pages 141–144, Karlskrona, Sweden, Juni 14-17, 1999.

[17] P. D. Holm. A new heuristic UTD diffraction coefficient for nonperfectly conducting wedges. *IEEE Trans. Antennas Propagat.*, AP-48(8):1211–1219, Aug. 2000.

FOI, Swedish Defence Research Agency, is a mainly assignment-funded agency under the Ministry of Defence. The core activities are research, method and technology development, as well as studies conducted in the interests of Swedish defence and the safety and security of society. The organisation employs approximately 1000 personnel of whom about 800 are scientists. This makes FOI Sweden's largest research institute. FOI gives its customers access to leading-edge expertise in a large number of fields such as security policy studies, defence and security related analyses, the assessment of various types of threat, systems for control and management of crises, protection against and management of hazardous substances, IT security and the potential offered by new sensors.

FOI
Swedish Defence Research Agency
SE-164 90 Stockholm

Phone: +46 8 555 030 00
Fax: +46 8 555 031 00

www.foi.se